



Strong slowing down of the thermalization of solids interacting in the extreme near field

M. Reina , R. Messina, and P. Ben-Abdallah *

*Laboratoire Charles Fabry, UMR 8501, Institut d'Optique, CNRS, Université Paris-Saclay,
2 Avenue Augustin Fresnel, 91127 Palaiseau Cedex, France*



(Received 28 June 2021; revised 30 August 2021; accepted 13 September 2021; published 27 September 2021)

When two solids at different temperatures are separated by a vacuum gap they relax toward their equilibrium state by exchanging heat either by radiation or by phonon or electron tunneling, depending on their separation distance and on the nature of materials. The interplay between this exchange of energy and its spreading through each solid entirely drives the relaxation dynamics. Here we highlight a significant slowing-down of this process in the extreme near-field regime at distances where the heat flux exchanged between the two solids is comparable or even dominates over the flux carried by conduction inside each solid. This mechanism, leading to a strong effective increase in the system thermal inertia, should play an important role in the temporal evolution of the thermal state of interacting solid systems at nanometric and subnanometric scales.

DOI: [10.1103/PhysRevB.104.L100305](https://doi.org/10.1103/PhysRevB.104.L100305)

The relaxation of bodies in mutual interaction which are initially prepared in two different thermal states is an important problem in physics from both a fundamental [1–10] and a practical point of view [11–17]. When these bodies are separated by a vacuum gap this relaxation is mediated by radiative heat exchange or by tunneling of heat carriers (phonons, electrons, excitons, etc.). Usually the system evolves toward a state of equipartition of energy and uniform temperature by maximizing its entropy [18]. This corresponds to an evolution of all particles inside the system toward the same average energy through various interaction mechanisms even if their initial energies are very different. This evolution is well described for classical systems by the Boltzmann equation for the probability density of particles, over all their possible states in the phase space.

In this paper we investigate the relaxation dynamics of systems exchanging heat in a strong-interaction regime. To explore this thermalization process we consider two solids out of thermal equilibrium which exchange heat through a nanometric or subnanometric vacuum gap in the transition domain between the radiative and the conductive regime [19–21] also called the extreme near-field regime. In this range of separation distance energy exchange competes or even dominates [22,23] with respect to the conductive heat transport within the bodies themselves. In this regime of strong interaction we demonstrate that counterintuitively the relaxation time of the system is dramatically extended compared to a weak-coupling situation and demonstrate that the relaxation time of the system towards thermal equilibrium is dramatically extended.

To address this problem let us consider two identical solid films as sketched in Fig. 1. When the heat transport inside these films is governed by a simple diffusion process the spatiotemporal evolution of the film temperature can be obtained

by solving the energy balance equation

$$\rho C \frac{\partial T_k(z, t)}{\partial t} = -\nabla \cdot [\kappa \nabla T_k(z, t)] + P^{j \rightarrow k}(z, t), \quad (1)$$

where ρ denotes the mass density of the films, C their specific heat capacity, κ their thermal conductivity, and $P^{j \rightarrow k}(z, t)$ the power density received locally by one film from the opposite one. This power density, as expected, depends implicitly on the entire temperature profiles $T_k(z, t)$ at each time t . It is clear that the time evolution of the temperature depends on the interplay between the inner transport mechanism and the heat exchange between the two films. When the flux carried by conduction within the films dominates with respect to the flux exchanged between the two films, the temperature profiles stay uniform at any time within each film and then the two temperatures obey the equation

$$\rho C \frac{dT_k}{dt} = P^{j \rightarrow k}[T_j(t), T_k(t)], \quad (2)$$

where now $P^{j \rightarrow k}[T_j(t), T_k(t)]$ corresponds to the total power (per unit volume) transferred from film j to film k , a function of the two temperatures T_j and T_k at time t . Close to thermal equilibrium the right-hand side of this equation can be expressed in terms of the radiative thermal conductance

$$G = \lim_{\Delta T \rightarrow 0} \frac{\phi^{j \rightarrow k}[T_k(t) + \Delta T, T_k(t)]}{\Delta T}, \quad (3)$$

where $\phi^{j \rightarrow k}$ is the net flux (per unit area) received by film k . This allows us to recast Eq. (2) in the form

$$\rho C L \frac{dT_k}{dt} = -G[T_k(t) - T_j(t)]. \quad (4)$$

If we assume (see Fig. 1) that body 2 is in contact with a thermostat at constant temperature T_2 , the only temperature varying in time is T_1 , which simply evolves as

$$T_1(t) = T_1(0) \exp(-t/\tau), \quad (5)$$

*pba@institutoptique.fr

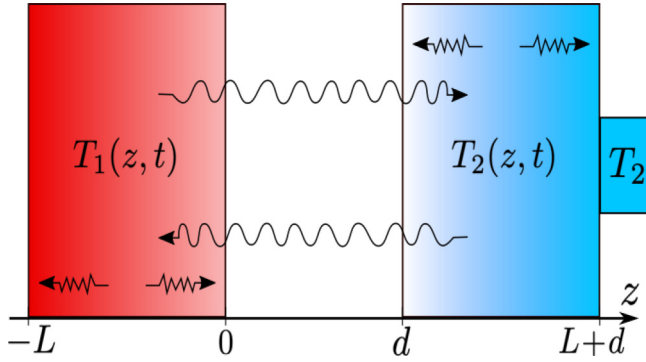


FIG. 1. Sketch of the system. Two solid films out of thermal equilibrium having temperatures $T_1(z, t)$ and $T_2(z, t)$ are separated by a vacuum gap of thickness d . They relax by exchanging heat either by radiation or by phonon or electron tunneling, depending on the separation distance and the nature of the materials. This transmitted energy is spread out through the films thanks to a diffusion process.

where $T_1(0)$ is the initial value of the temperature of slab 1, and $\tau = \rho CL/G$ denotes the relaxation time. Hence we see that one way to slow down the thermalization process consists in reducing the coupling strength between the two films, encoded in the conductance G . In the following, we show that a strong slowing-down of the relaxation process can also be observed in some situations when the energy exchange between the two films is strongly coupled to the conduction mechanism within each one of them.

To demonstrate this result let us first consider the relaxation of two polar films separated by a gap of nanometric thickness. At this separation distance the films interact only by radiation through the tunneling of evanescent photons [24]. The radiative power density $P_r^{j \rightarrow k}$ dissipated in film k at point z and associated with the sources in the other body can be calculated from the average monochromatic flux of the Poynting vector at this point, $\langle \mathbf{S}^k(z, \omega) \rangle = 2 \text{Re}(\mathbf{E}^k(z, \omega) \times \mathbf{H}^{k*}(z, \omega))$, as

$$P_r^{j \rightarrow k}(z) = - \int_0^\infty d\omega \nabla \cdot \langle \mathbf{S}^k(z, \omega) \rangle, \quad (6)$$

where $\langle \cdot \rangle$ denotes the statistical averaging. According to fluctuational-electrodynamics theory [25], for isotropic media and neglecting nonlocal effects, the Poynting vector reads

$$\langle \mathbf{S}_n^k(z, \omega) \rangle = i \frac{\omega^2}{c^2} \eta_{njl} \times \int_{\text{sources}} dz' \epsilon''(z', \omega) \Theta[T(z'), \omega] \mathbb{G}_{j,l}^{EE} \mathbb{G}_{n,l}^{HE*}, \quad (7)$$

where the integral extends over all source points. In Eq. (7), η_{njl} denotes the njl component of the Levi-Civita tensor, $\Theta(T, \omega) = \hbar\omega/[e^{\hbar\omega/k_B T} - 1]$ is the mean energy of a Planck oscillator at temperature T , ϵ'' the imaginary part of the permittivity in the emitting body, and $\mathbb{G}^{EE} = \mathbb{G}^{EE}(z, z')$ and $\mathbb{G}^{HE} = \mathbb{G}^{HE}(z, z')$ are the full electric-electric and electric-magnetic dyadic Green tensors [26] at frequency ω , taking into account all scattering events within the system between the emitter and the point where energy is dissipated.

As recently established [23] the radiative power dissipated through a polar film from its surface is typically reduced by one order of magnitude through a distance of a few nanometers from the vacuum gap, so that the radiative transfer can reasonably be assumed to be purely surfacic. In this case, by assuming the thermal conductivity independent of the position and the temperature and by introducing the auxiliary functions $F_k(z, t) = T_k(z, t) - T_2$, the energy balance equation can be recast in the form

$$\rho CL \frac{\partial F_k(z, t)}{\partial t} = -\kappa L \frac{\partial^2 F_k(z, t)}{\partial z^2} + G_r F_k(z, t), \quad (8)$$

where in this scenario the conductance between the two films reduces to the radiative conductance G_r , defined as

$$G_r = \int_0^\infty \frac{d\omega}{2\pi} \frac{d\Theta(T, \omega)}{dT} \sum_p \int_0^\infty \frac{dk_{\parallel}}{2\pi} k_{\parallel} \mathcal{T}_p(\omega, k_{\parallel}, d), \quad (9)$$

where k_{\parallel} is the modulus of the component of the wave vector parallel to the exchange surface and p is the state of polarization. Here $\mathcal{T}_p(\omega, k_{\parallel}, d)$ denotes the energy transmission coefficient for the mode (ω, k_{\parallel}) in polarization p between the films, which can be expressed in terms of the reflection and transmission coefficients r_{ip} and t_{ip} of the two slabs as [24]

$$\mathcal{T}_p(\omega, k_{\parallel}, d) = \begin{cases} \frac{(1-|r_{1p}|^2-|t_{1p}|^2)(1-|r_{2p}|^2-|t_{2p}|^2)}{|D_p|^2}, & ck_{\parallel} < \omega, \\ \frac{4 \text{Im}(r_{1p}) \text{Im}(r_{2p}) e^{-2|k_z|d}}{|D_p|^2}, & ck_{\parallel} > \omega, \end{cases} \quad (10)$$

k_z being the z component of the wave vector and $D_p = 1 - r_{1p}r_{2p}e^{2ik_z d}$ the Fabry-Pérot factor of the cavity.

As for the initial conditions, we impose $F_1(z, 0) = \Delta T$ and $F_2(z, 0) = 0$, which correspond to the fact that the initial temperature profiles in the two slabs are uniform [$T_1(z, 0) = T_2 + \Delta T$ and $T_2(z, 0) = T_2$]. Concerning the boundary conditions, we set $F_2(L+d, t) = 0$, fixing the temperature at T_2 for the edge of the right slab in contact with the thermostat, while $\partial_z F_1(-L, t) = 0$ imposes a vanishing flux at each instant at the left end of the first slab (adiabatic boundary condition). Note that this condition is based on the fact that the interactions in the far-field regime with the bath are negligible when the distance d between the slabs is in the near-field regime. Moreover, we impose two further boundary conditions, $\partial_z F_1(0, t) = -G_r/\kappa [F_1(0, t) - F_2(d, t)]$ and $\partial_z F_2(d, t) = -G_r/\kappa [F_1(0, t) - F_2(d, t)]$, ensuring the flux continuity between the two slabs. The solutions of the partial differential equations, (8), read

$$\begin{aligned} F_1(z, t) &= 8\Delta T \sum_{n=1}^{\infty} \frac{\sin x_n \cos^2 x_n}{4x_n + \sin(4x_n)} \\ &\quad \times \cos\left[\frac{x_n(z+L)}{L}\right] \exp\left[-\frac{x_n^2 \kappa}{\rho CL^2} t\right], \\ F_2(z, t) &= -8\Delta T \sum_{n=1}^{\infty} \frac{\sin^2 x_n \cos x_n}{4x_n + \sin(4x_n)} \\ &\quad \times \sin\left(\frac{x_n z}{L}\right) \exp\left[-\frac{x_n^2 \kappa}{\rho CL^2} t\right], \end{aligned} \quad (11)$$

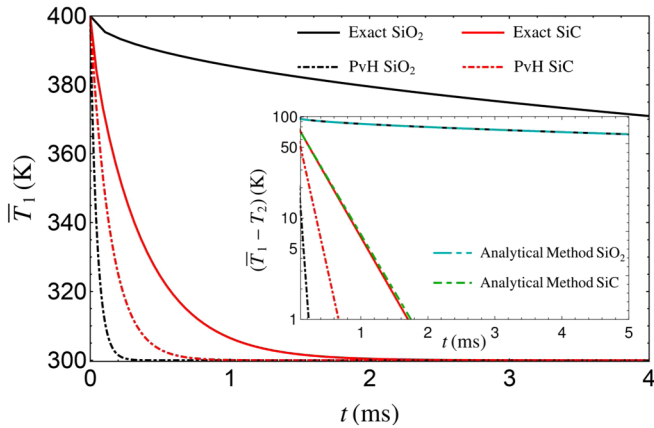


FIG. 2. Time evolution of the average temperature of the hot film in a system made of two coupled polar films of thickness $L = 100 \mu\text{m}$ separated by a vacuum gap of thickness $d = 1 \text{ nm}$. The black (red) solid curve shows the evolution for SiO_2 (SiC) coupled films. The black (red) dashed curves show the evolution predicted by the PvH theory (perfectly conducting solids). The initial temperature of the cold film is $T_2 = 300 \text{ K}$ and the initial temperature difference is $\Delta T = 100 \text{ K}$. The mass density, the specific heat, and the thermal conductivity of SiC and SiO_2 are $\rho_{\text{SiC}} = 3200 \text{ kg} \cdot \text{m}^{-3}$, $C_{\text{SiC}} = 600 \text{ J} \cdot \text{kg}^{-1} \cdot \text{K}^{-1}$, $\rho_{\text{SiO}_2} = 2650 \text{ kg} \cdot \text{m}^{-3}$, $C_{\text{SiO}_2} = 680 \text{ J} \cdot \text{kg}^{-1} \cdot \text{K}^{-1}$, $\kappa_{\text{SiC}} = 120 \text{ W} \cdot \text{m}^{-1} \cdot \text{K}^{-1}$, and $\kappa_{\text{SiO}_2} = 1.2 \text{ W} \cdot \text{m}^{-1} \cdot \text{K}^{-1}$.

where x_n are the solutions of the transcendental equation $x \tan 2x = 2G_r L / \kappa$. We can associate each term with a partial relaxation time $\tau_n = \rho C L^2 / (x_n^2 \kappa)$. It can be easily shown that $x_1 < x_n$ and thus $\tau_1 > \tau_n$ for all $n \geq 2$, so that the first term in these series is the dominant one for large t . The ratio GL/κ quantifies the relative importance of the radiative and conductive transport [for two silicon carbide (SiC) films this ratio is 1.1, while it increases to 312.5 for two silica (SiO_2) films]. The appearance of the ratio GL/κ as a key parameter allows us to anticipate a reduction of the effect when reducing the slab thickness L or when increasing the separation distance d (coupling strength) between them (see Supplemental Material [27]).

When the heat transport by conduction is much more efficient than the transport by radiation, the temperature within each film is almost uniform at any time. In this case the solution of Eq. (8) is similar to that of Eq. (4) and the temperature profile is the same as the one predicted by the Polder and van Hove (PvH) theory of radiative heat transfer between perfectly conducting solids. However, the situation radically changes when the magnitude of radiative heat transfer is comparable to or even larger than the heat transfer by conduction within the films. In Fig. 2 we compare the time evolution of the mean temperature $\bar{T}_1(t) = (1/L) \int T_1(z, t) dz$ inside the left (hot) slab obtained by solving Eq. (1) by means of a finite-difference method [27] to the predictions from the PvH theory for SiC and SiO_2 films. It can be noted that the deviation between the two temperature profiles is more pronounced for two SiO_2 slabs compared to SiC slabs. As anticipated previously, this is due to the fact that the thermal conductivities of SiC and SiO_2 samples are strongly different. The relatively small conductivity of SiO_2 leads to a strong deviation from the

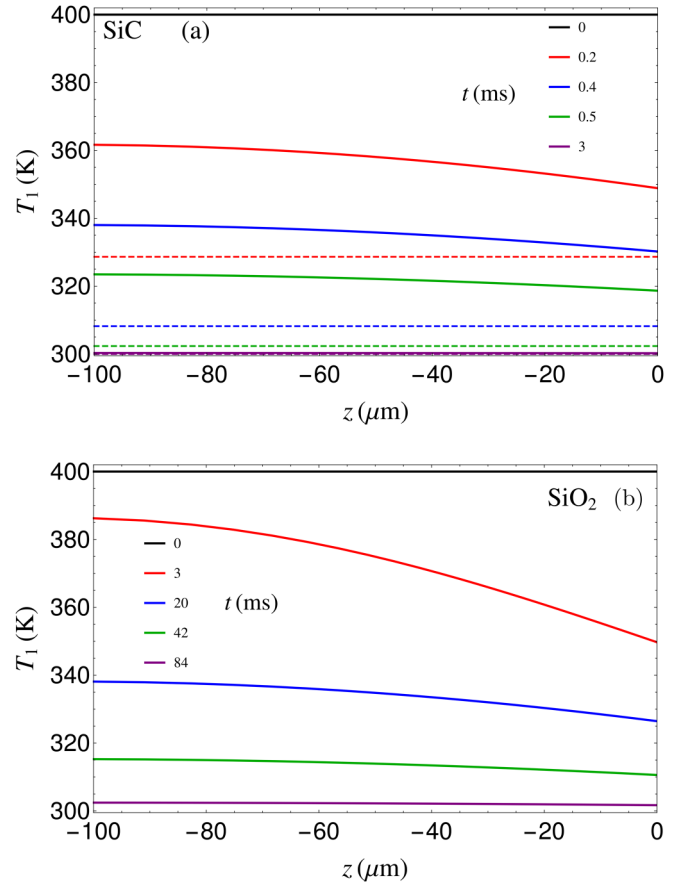


FIG. 3. Temperature profile as a function of time in the hot film of a system made of two coupled polar films of thickness $L = 100 \mu\text{m}$. Dashed lines correspond to the temperature predicted by the PvH theory. (a) SiC films separated by a 1-nm-thick vacuum gap. (b) The same configuration with SiO_2 films.

PvH predictions. Moreover, as shown in the inset in Fig. 2, we see that the time evolution of $\bar{T}_1 - T_2$ is exponentially decaying as predicted by the analytical solution, (11), and the decay rate of the temperature corresponds to the relaxation time τ_1 . Note also that the comparison in the inset of the solution of Eq. (8) with the exact solution of Eq. (1) obtained using a finite-difference method demonstrates that the near-field radiative transfer is indeed a surface phenomenon. As shown in the inset in Fig. 2, the relaxation dynamics is more than one order of magnitude slower when the near-field heat transfer is comparable to the conductive transfer inside the films, showing that the coupling acts as an additional source of thermal inertia. Actually, at the macroscopic level the coupling mechanism tends to increase the thermal inertia of the system by decreasing its effective diffusivity $D_n = x_n^2 \kappa / (\rho C)$. At a more microscopic level, the power dissipated by photons inside the atomic lattice is comparable to or even larger than the one dissipated by phonons, thus leading to a longer relaxation time.

As far as the temperature profile is concerned, we see in Fig. 3 that it differs from the uniform profile, especially when the radiative transfer dominates with respect to the conductive transport, as in the configuration of coupled SiO_2 films. As we can see, a nonnegligible temperature profile appears through

the slab because of the diffusion process in both materials. Although the heat spreads inside the films by conduction, the temperature profiles are, of course, not linear because of the interplay between the diffusion process and the near-field heat transfer. For SiC films we also show (dashed lines) the value T_{PvH} of the (uniform) temperature predicted by the PvH model at the same moments, while for SiO₂ this comparison has been omitted since in this case the two relaxation processes take place at two very different time scales, as shown in Fig. 2. Indeed in this case, after only 0.2 ms the hot film is already thermalized according to the predictions of PvH theory, while a hundredfold longer time is required when the near-field radiative heat exchange is competing with the diffusion process.

So far we have limited ourselves to a transfer between the two solids mediated by photon tunneling. We now consider the thermalization process in the case of two metallic films interacting through electron tunneling. In fact, it has been recently shown [28] that in this scenario the flux carried by electrons at subnanometric distances surpasses by several orders of magnitude the flux carried by photons and can therefore surpass the conductive (phononic) flux inside the metals. The electronic thermal conductance due to electron tunneling can be easily calculated using the effective potential barrier associated with the vacuum gap between the two metals. For two identical metals without bias voltage applied through the system the effective potential is a simple rectangular barrier and the transmission probability $\mathcal{T}(E_z, d)$ at distance d of electrons of normal energy E_z through this barrier reads [29]

$$\mathcal{T}(E_z, d) = \frac{4E_z(E_z - V)}{4E_z(E_z - V) + V^2 \sin^2(k_{2z}(E_z, V)d)}, \quad (12)$$

where $k_{2z}(E_z, V) = \sqrt{2m_e(E_z - V)}/\hbar$ denotes the normal components of the wave vector inside the gap (m_e being the electron mass) and the barrier height is written here as $V(d) = V_{\text{ev}}(d) + E_F$, E_F being the Fermi energy ($E_F = 5.53$ eV for gold) and V_{ev} a distance-dependent function for which the data taken from [30] have been fitted from DFT calculations with the log-scale law $V_{\text{ev}}(d) = V_0 \ln(1 + d/1 \text{ \AA})$ ($V_0 = 1.25$ eV for gold). It follows that the heat flux carried by electrons by the tunneling effect can be calculated by summing over all energies E_z in the direction normal to the surface. This allows us to define the electronic heat conductance as

$$G_e = \int_0^\infty dE_z E_z \frac{\partial N(E_z, T)}{\partial T} \mathcal{T}(E_z, d), \quad (13)$$

where $N(E_z, T)dE_z$, with $N(E_z, T) = \frac{m_e k_B T}{2\pi^2 \hbar^3} \ln[1 + \exp(-(E_z - E_F)/k_B T)]$, denotes the number of electrons in the metal at temperature T with a normal energy between E_z and $E_z + dE_z$ across a unit area per unit time.

This conductance can reach values about six orders of magnitude larger than G_r for gold films at separation distances of a few angstroms [28]. In the presence of electron tunneling, the energy-balance equation, (8), remains valid, provided that the permutation $G_r \leftrightarrow G_e$ is made. For two gold films, the ratio $G_e L/\kappa$ equals 2.1, 306.5, and 871 for separation distances $d = 5 \text{ \AA}$, $d = 2 \text{ \AA}$ and $d = 1 \text{ \AA}$, respectively. This suggests a strong effect of the coupling mechanism on the relaxation dynamics. In Fig. 4 we compare the time evolution of the average temperature profile for the hot film in a system of two gold films with and without coupling between heat

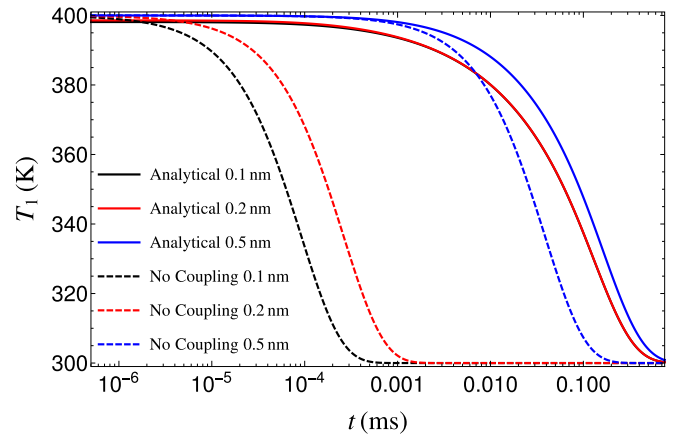


FIG. 4. Time evolution of the average temperature of the hot film in a system made up of two coupled gold films of thickness $L = 100 \mu\text{m}$ at subnanometric distances and comparison with the temperature evolution (dashed curves) without coupling. The initial temperature of the cold film is $T_2 = 120$ K and the initial temperature difference is $\Delta T = 160$ K. The gold mass density is $\rho = 19\,300 \text{ kg} \cdot \text{m}^{-3}$ and its specific heat capacity is $C = 128 \text{ J} \cdot \text{kg}^{-1} \cdot \text{K}^{-1}$.

conduction and heat transfer by electron tunneling. Unlike polar films interacting by radiation, here the relaxation process toward thermal equilibrium is much faster, by two orders of magnitude. But more interesting is the impact of coupling on the relaxation time. At a distance $d = 5 \text{ \AA}$ ($G_e L/\kappa = 2.1$) this difference between the scenarios with and those without coupling is relatively modest and the coupling slows down the thermalization process by a factor of approximately 2. On the other hand, at closer separation distances this slowdown becomes remarkable, reaching about three orders of magnitude. Note that for these distances the temporal evolutions of the average temperatures are almost indistinguishable (solid red and black curves) since the x_n in solution (11) of the energy-balance equation, (8), are really close to the asymptotic value (i.e., large value of $G_e L/\kappa$).

In conclusion, we have demonstrated a strong impact of the interplay between the heat transfer in the extreme near-field regime between two solids and the heat spreading mechanism by conduction inside these media. When the thermal conductance of heat exchange through the separation gap is comparable to or dominates the conductance associated with the diffusive process inside the solids, the thermalization of these media is greatly slowed down. In this case the relaxation time can be longer even by several orders of magnitude than in the classical situation where conduction is the dominant mechanism. This effect should play an important role in the fields of active thermal management at nanoscale, pyroelectric energy conversion in the extreme near-field regime, and nanoscale heat engines or for the Boolean treatment of information with heat at nanoscale. In this preliminary work we were limited to the study of the relaxation process by assuming that the optical response of materials is local. In further works the role of the nonlocal behavior of this response in the relaxation dynamics will have to be studied.

P. B.-A. acknowledges discussions with S.-A. Biehs of Carl von Ossietzky Universität, Germany.

- [1] D. J. Evans, D. J. Searles, and S. R. Williams, Dissipation and the relaxation to equilibrium, *J. Stat. Mech.: Theory Exp.* (2009) P07029.
- [2] H. G. Schuster, *Deterministic Chaos: An Introduction* (Wiley, New York, 1995).
- [3] I. Prigogine, *From Being to Becoming: Time and Complexity in the Physical Sciences* (Freeman, San Francisco, 1980).
- [4] F. Jin, T. Neuhaus, K. Michielsen, S. Miyashita, and M. Novotny, Equilibration and thermalization of classical systems, *New J. Phys.* **15**, 033009 (2013).
- [5] J. C. Reid, D. J. Evans, and D. J. Searles, Beyond Boltzmann's H-theorem: Demonstration of the relaxation theorem for a non-monotonic approach to equilibrium, *J. Chem. Phys.* **136**, 021101 (2012).
- [6] R. Messina, M. Tschikin, S.-A. Biehs, and P. Ben-Abdallah, Fluctuation-electrodynamics theory and dynamics of heat transfer in systems of multiple dipoles, *Phys. Rev. B* **88**, 104307 (2013).
- [7] P. Ben-Abdallah, R. Messina, S.-A. Biehs, M. Tschikin, K. Joulain, and C. Henkel, Heat Superdiffusion in Plasmonic Nanostructure Networks, *Phys. Rev. Lett.* **111**, 174301 (2013).
- [8] I. Latella, S.-A. Biehs, R. Messina, A. W. Rodriguez, and P. Ben-Abdallah, Ballistic near-field heat transport in dense many-body systems, *Phys. Rev. B* **97**, 035423 (2018).
- [9] S. Sanders, L. Zundel, W. J. M. Kort-Kamp, D. A. R. Dalvit, and A. Manjavacas, Near-Field Radiative Heat Transfer Eigenmodes, *Phys. Rev. Lett.* **126**, 193601 (2021).
- [10] S. Sadasivam, M. K. Y. Chan, and P. Darancet, Theory of Thermal Relaxation of Electrons in Semiconductors, *Phys. Rev. Lett.* **119**, 136602 (2017).
- [11] B. Guha, C. Otey, C. B. Poitras, S. Fan, and M. Lipson, Near-field radiative cooling of nanostructures, *Nano Lett.* **12**, 4546 (2012).
- [12] S. A. Dyakov, J. Dai, M. Yan, and M. Qiu, Thermal radiation dynamics in two parallel plates: The role of near field, *Phys. Rev. B* **90**, 045414 (2014).
- [13] P. Ben-Abdallah and S.-A. Biehs, Towards Boolean operations with thermal photons, *Phys. Rev. B* **94**, 241401(R) (2016).
- [14] K. Chen, P. Santhanam, and S. Fan, Near-Field Enhanced Negative Luminescent Refrigeration, *Phys. Rev. Applied* **6**, 024014 (2016).
- [15] R. Yu, A. Manjavacas, and F. J. García de Abajo, Ultrafast radiative heat transfer, *Nat. Commun.* **8**, 1 (2017).
- [16] I. Latella, O. Marconot, J. Sylvestre, L. G. Fréchet, and P. Ben-Abdallah, Dynamical Response of a Radiative Thermal Transistor Based on Suspended Insulator-Metal-Transition Membranes, *Phys. Rev. Applied* **11**, 024004 (2019).
- [17] B. Bhatia, H. Cho, J. Karthik, J. Choi, D. G. Cahill, L. W. Martin, and W. P. King, High power density pyroelectric energy conversion in nanometer-thick BaTiO₃ films, *Nanoscale Microscale Thermophys. Eng.* **20**, 137 (2016).
- [18] R. Kubo, M. Toda, and N. Hashitsume, *Statistical Physics II: Nonequilibrium Statistical Mechanics*, Springer Series in Solid-State Science Vol. 31 (Springer, New York, 1985).
- [19] V. Chiloyan, J. Garg, K. Esfarjani, and G. Chen, Transition from near-field thermal radiation to phonon heat conduction at sub-nanometre gaps, *Nat. Commun.* **6**, 6755 (2015).
- [20] K. Kim, B. Song, V. Fernández-Hurtado, W. Lee, W. Jeong, L. Cui, D. Thompson, J. Feist, M. T. H. Reid, F. J. García-Vidal, J. C. Cuevas, E. Meyhofer, and P. Reddy, Radiative heat transfer in the extreme near field, *Nature (London)* **528**, 387 (2015).
- [21] K. Kloppstech, N. Köne, S.-A. Biehs, A. W. Rodriguez, L. Worbes, D. Hellmann, and A. Kittel, Giant heat transfer in the crossover regime between conduction and radiation, *Nat. Commun.* **8**, 14475 (2017).
- [22] R. Messina, W. Jin, and A. W. Rodriguez, Strongly coupled near-field radiative and conductive heat transfer between planar bodies, *Phys. Rev. B* **94**, 121410(R) (2016).
- [23] M. Reina, R. Messina, and P. Ben-Abdallah, Conduction-Radiation Coupling Between Two Closely-Separated Solids, *Phys. Rev. Lett.* **125**, 224302 (2020).
- [24] D. Polder and M. van Hove, Theory of radiative heat transfer between closely spaced bodies, *Phys. Rev. B* **4**, 3303 (1971).
- [25] S. M. Rytov, Y. A. Kravtsov, and V. I. Tatarskii, *Principles of Statistical Radiophysics*, Vol. 3 (Springer, New York, 1989).
- [26] M. S. Tomaš, Green function for multilayers: Light scattering in planar cavities, *Phys. Rev. A* **51**, 2545 (1995).
- [27] See Supplemental Material at <http://link.aps.org/supplemental/10.1103/PhysRevB.104.L100305> for a description of the finite-difference method used to solve Eq. (1) and of the dependence of the mean temperature of films on their separation distance and on their thickness.
- [28] R. Messina, S.-A. Biehs, T. Ziehm, A. Kittel, and P. Ben-Abdallah, Heat transfer between two metals through subnanometric vacuum gaps, [arXiv:1810.02628](https://arxiv.org/abs/1810.02628).
- [29] C. Cohen-Tannoudji, J. Dupont-Roc, and G. Grynberg, *Atom-Photon Interactions* (Wiley, New York, 1992).
- [30] A. Kiejna, Potential barrier for the metal-vacuum-metal tunneling electrons, *Ultramicroscopy* **42**, 231 (1992).